Non-oxo vanadium(IV) alkoxide chemistry: solid state structures, aggregation equilibria and thermochromic behaviour in solution

Kátia C. M. Westrup,[a] Thaiane Gregório,[a] Danilo Stinghen,[a] Dayane M. Reis,[a] Peter B. Hitchcock,[b] Ronny R. Ribeiro,[a] Andersson Barison,[a] Davi F. Back,[c] Eduardo L. De Sá,[a] Giovana G. Nunes[a] and Jaísa F. Soares*[a]

[a] *Departamento de Química, Universidade Federal do Paraná, Centro Politécnico, 81530-900 – Curitiba-PR, Brazil. Fax: +55 41 33613186; Tel: +55 41 33613180; E-mail: jaisa.soares@ufpr.br*

[b] *Department of Chemistry, University of Sussex, Brighton BN1 9QJ, UK*

[c] *Departamento de Química, Universidade Federal de Santa Maria, Camobi, 97105-900 – Santa Maria-RS, Brazil*

Experimental details

EPR spectroscopy. Crystalline samples were dissolved in toluene or hexane for solution studies at variable temperature or powdered for analysis in the solid state. 77 K experiments were carried out by means of a quartz insertion finger Dewar. Signal channel field modulation amplitude was adjusted to less than 10% of the smallest linewidth to safely improve signal-to-noise ratio, while signal channel time constant was set to less than 10% of the conversion time to avoid distortion effects. Microwave power was set bellow saturation.

Synthesis of $[V_2(\mu\text{-}OBu^s)_2(OBu^s)_6]$ (complex B^s). A 250 mL Schlenk flask containing 40 mL of thf, 120 mL of hexane and 4.14 g (51.0 mmol) of $LiOBu^s$ was connected to a reflux condenser through a pressure-equalized glass column fitted with a glass sintered plate. $[VCl_3(thf)_3]$ (4.61 g, 12.3 mmol) was placed on the plate and slowly extracted by the condensing solvents into the boiling $LiOBu^s$ solution. When the extraction was complete, the reaction mixture (purple solution + white solid in suspension) was cooled down to the room temperature, received the addition of 1.6 g (16.0 mmol) of CuCl and was heated again under reflux for 3-4 h, producing a blue-green solution with red-brownish copper(0) powder in suspension. The solid was filtered off and the reaction mixture was evaporated under vacuum to half volume, filtered again through Celite and then evaporated to constant weight. Yield: 2.83 g, 68 %.

Synthesis of $[V(OPe^t)_4]$ (complex P^t).The general procedure was similar to the described for B^s, with 8.47 g (76.9 mmol) of sodium *tert*-pentoxide, 7.03 g (18.8 mmol) of $[VCl_3(thf)_3]$, 100 mL of hexane and 180 mL of thf. However, few minutes after the reaction mixture started boiling, the formation of a large amount of a purple solid was observed. In an unsuccessful attempt to

dissolve the powder, the volume of thf was gradually increased from the initial 30 mL to a total amount of 180 mL. In fact, the amount of solid appeared to increase after each addition of the solvent. The reaction mixture was then cooled down to room temperature and left stirring for 20 h, before receiving the addition of 100 more milliliters of hexane and of large excess of CuCl (5.07 g, 51.2 mmol). After 24 h under reflux, the purple powder remained in suspension and the supernatant was green. The mixture was decanted at room temperature for 4 days and then filtered. The solid (15.5 g) was dried under vacuum and the emerald-green liquid was filtered through Celite, evaporated under vacuum to remove all solvents and finally filtered again through Celite. Yield: 2.21 g (29 %) of P^t.

Results and Discussion

Thermochromic behaviour in solution

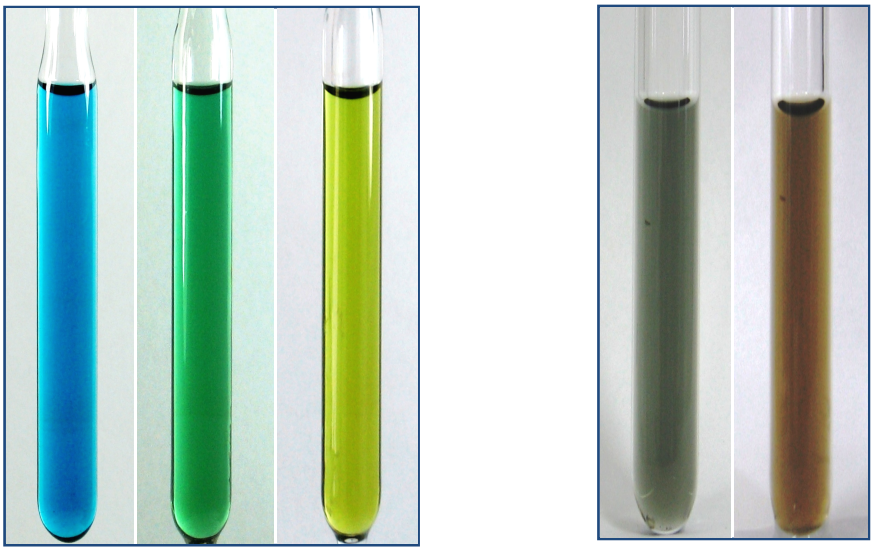

(a) (b)

Figure S1 – Colour changes in hexane solutions of (a) **C** and (b) $\mathbf{B}^s$ with varying temperature. For temperature intervals, see Table 1 in the main text.

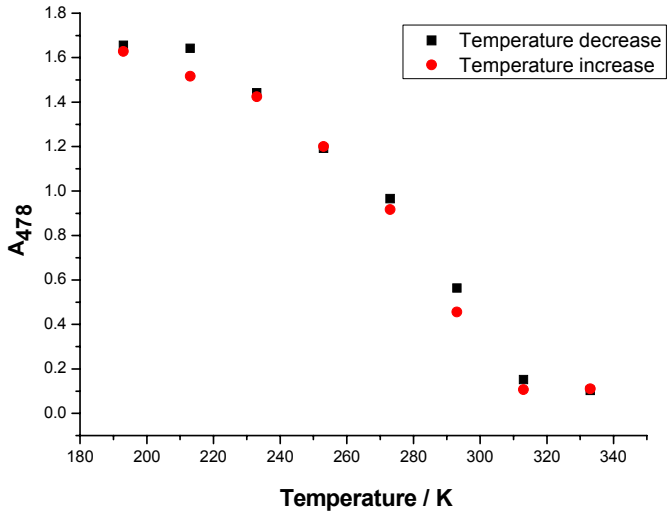

Figure S2 - Changes in absorbance registered at 478 nm for a hexane solution of **N** (9.3 x 10^{-3} mol L^{-1}) with varying temperature, evidencing the reversible character of the thermochromic behaviour.

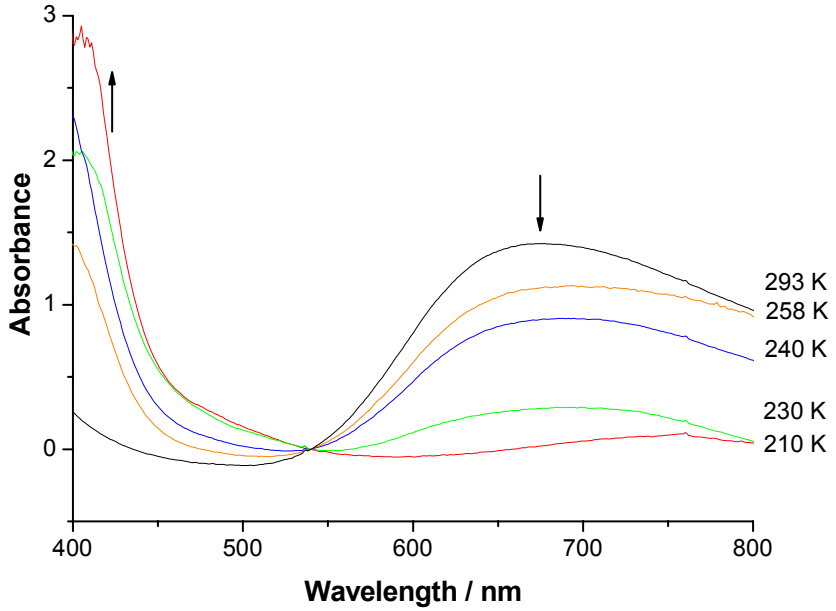

Figure S3 - Electronic spectra recorded for **C** in hexane solution (10 mmol L^{-1}). Arrows indicate intensity changes with decreasing temperature.

EPR spectroscopy

Correlation times and rotational radii for the mononuclear species in solution at room temperature

An intuitive arrangement of the rotational correlation times based on the molecular structures of the ligands follows a remarkable correlation with the calculated effective rotational radii, being the latter proportional to the former through the Stokes-Einstein relationship for spherical molecules in Brownian motion (Equation 2).[1]

$$\tau_c = \frac{4\pi\eta a^3}{3k_B T} \qquad (2)$$

where τ_c is the rotational correlation time, η is the solvent viscosity, k_B is the Boltzmann constant and *a* is the effective rotational radius. Hence, as expected, the effective rotational radius for **I** is the smallest and, for **C**, one of the largest.

Table S1 – EPR parameters from the room temperature solutions[(a)] (high temperature, mononuclear species)

Sample	Correlation time τ_c [x 10^{-12} s]	Rotational radius *a* [pm]
$\mathbf{B^t}$	4.108	188.8
$\mathbf{P^t}$	5.481	207.8
I	1.935	146.9
$\mathbf{B^s}$	3.393	177.1
N	3.702	182.3
C	4.209	190.3

([a]) Solution concentration = 10 mmol L^{-1} in toluene.

EPR spectra obtained for toluene solutions of C, $\mathbf{B}^{s}$ *and* $\mathbf{P}^{t}$ *(variable temperature and 77 K)*

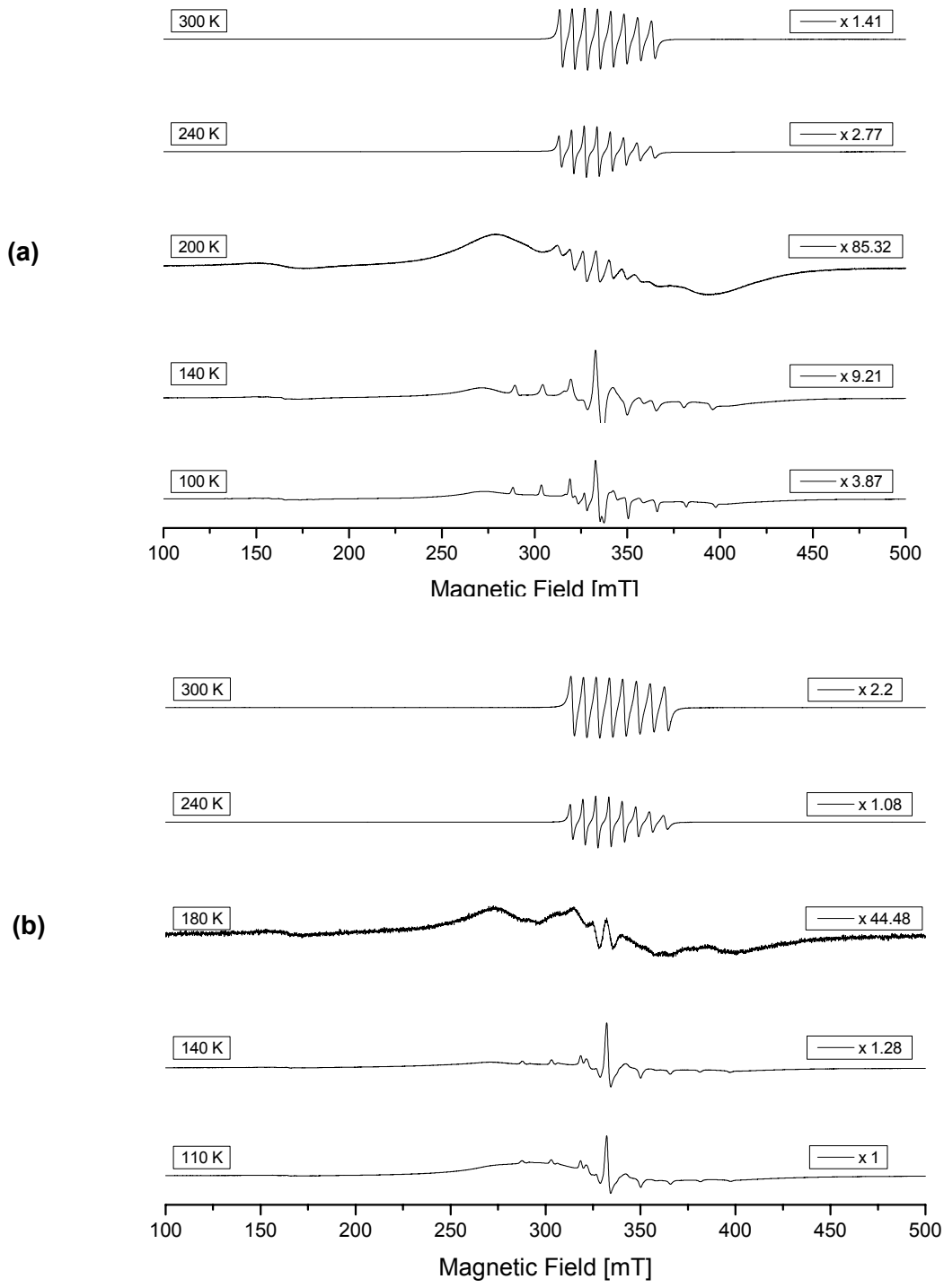

Figure S4 – Variable temperature EPR spectra registered for 10 mmol L^{-1} toluene solutions of (a) complex **C** and (b) complex $\mathbf{B}^{s}$. Temperatures are shown on the left hand side, while numbers on the right are normalization factors employed to draw similar intensity spectra.

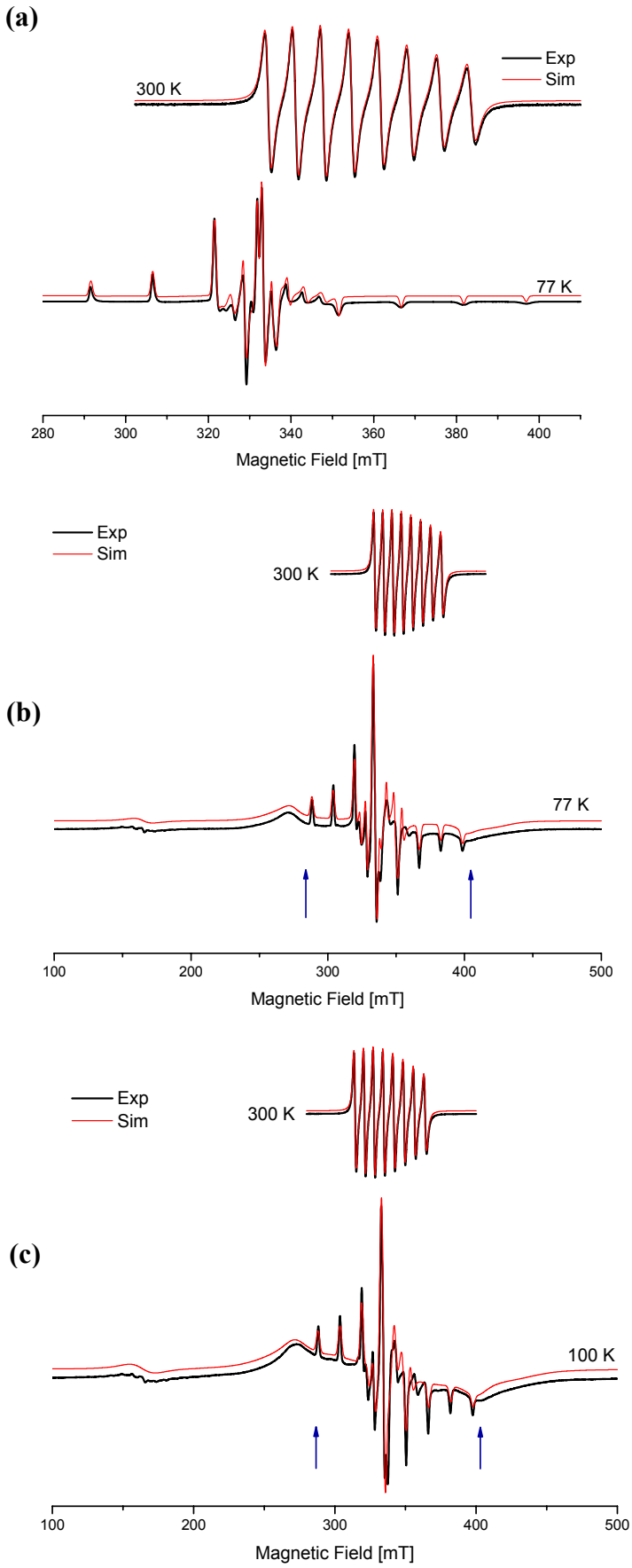

Figure S5 – Experimental (black lines) and simulated (red lines) EPR spectra registered for *(a)* complex $\mathbf{P}^{t}$; *(b)* complex $\mathbf{B}^{s}$ and *(c)* complex **C** at 300 (top) and 77 K (bottom). The calculated parameters presented in Tables 5, 6 and 7 were obtained from these simulated spectra, as well as from those shown in Figure 6. The sharp hyperfine lines delimited by the arrows in Figure S5(b,c) are probably generated by mononuclear species in equilibrium with the triplet form.

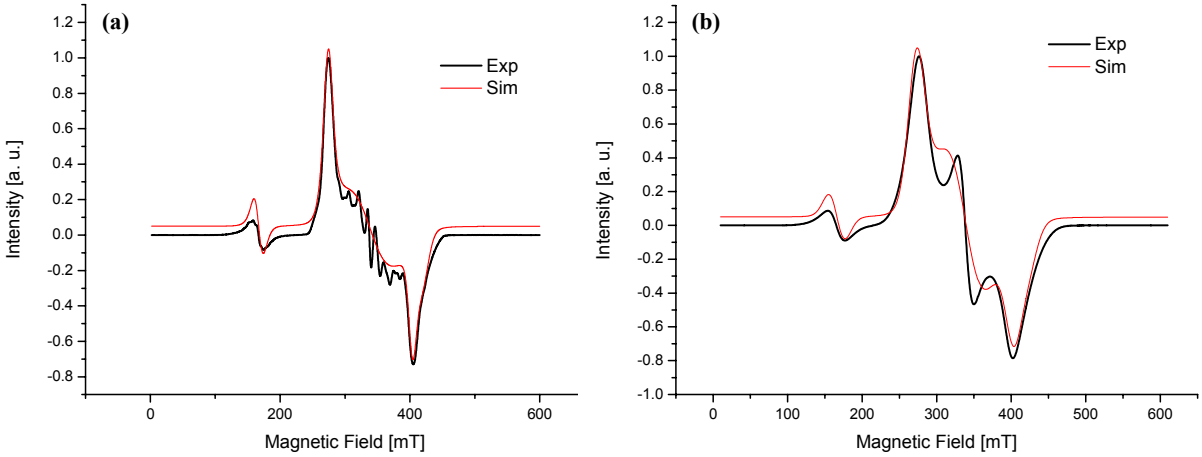

Figure S6 – Experimental (black lines) and simulated (red lines) EPR spectra for (a) complex **C** and (b) complex **I** in the solid state at 77 K.

EPR spectra of frozen solutions of complex N

Table S2 – EPR and zero-field parameters from the frozen solutions of **N** (quick freezing at 77 K)

Sample	*g*-Tensor				*D*-Tensor [cm^{-1}]	
	x	*y*	*z*	g_{iso}	*D*	*E*
N (species 1) **N** (species 2)	1.9740	1.9536	1.9335	1.9537	0.0772 0.2048	0.0140 0.0247

(a)

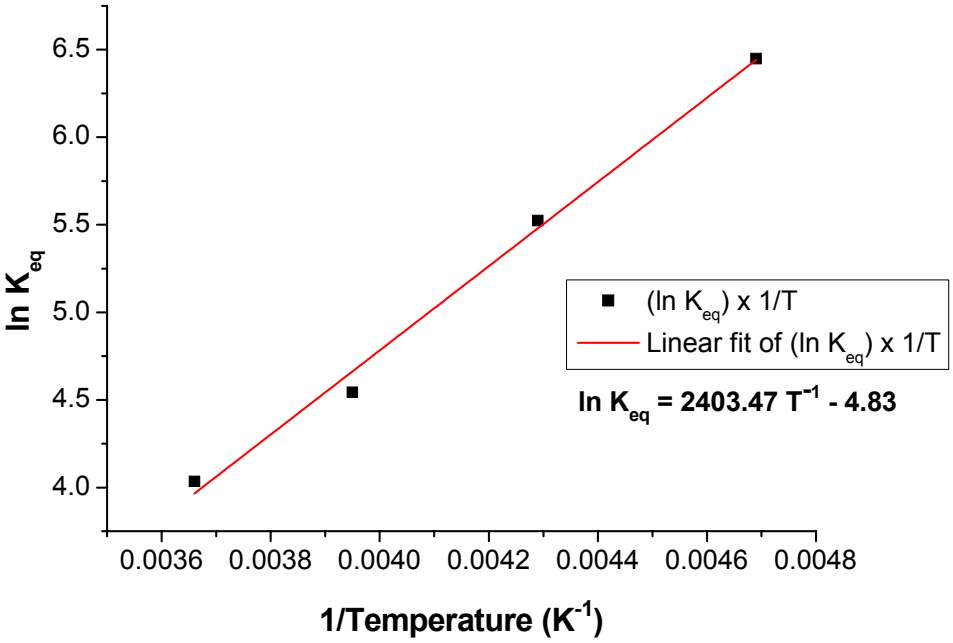
6.5
6.0
5.5
5.0
4.5
4.0
ln K_eq
0.0036
0.0038
0.0040
0.0042
0.0044
0.0046
0.0048
1/Temperature (K^-1)
(ln K_eq) x 1/T
Linear fit of (ln K_eq) x 1/T
ln K_eq = 2403.47 T^-1 - 4.83

(b)

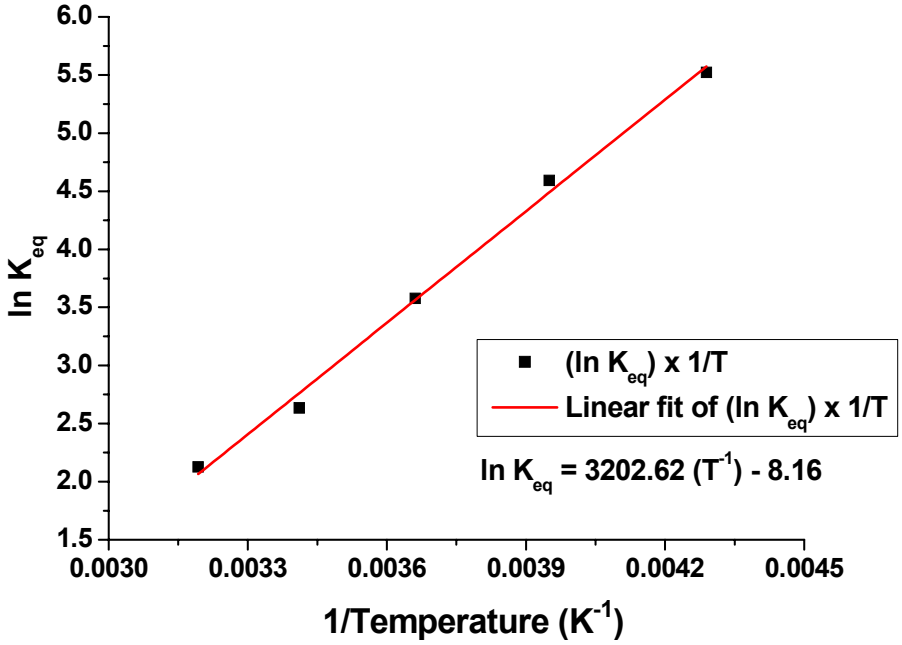
6.0
5.5
5.0
4.5
4.0
3.5
3.0
2.5
2.0
1.5
ln K_eq
0.0030
0.0033
0.0036
0.0039
0.0042
0.0045
1/Temperature (K^-1)
(ln K_eq) x 1/T
Linear fit of (ln K_eq) x 1/T
ln K_eq = 3202.62 (T^-1) - 8.16

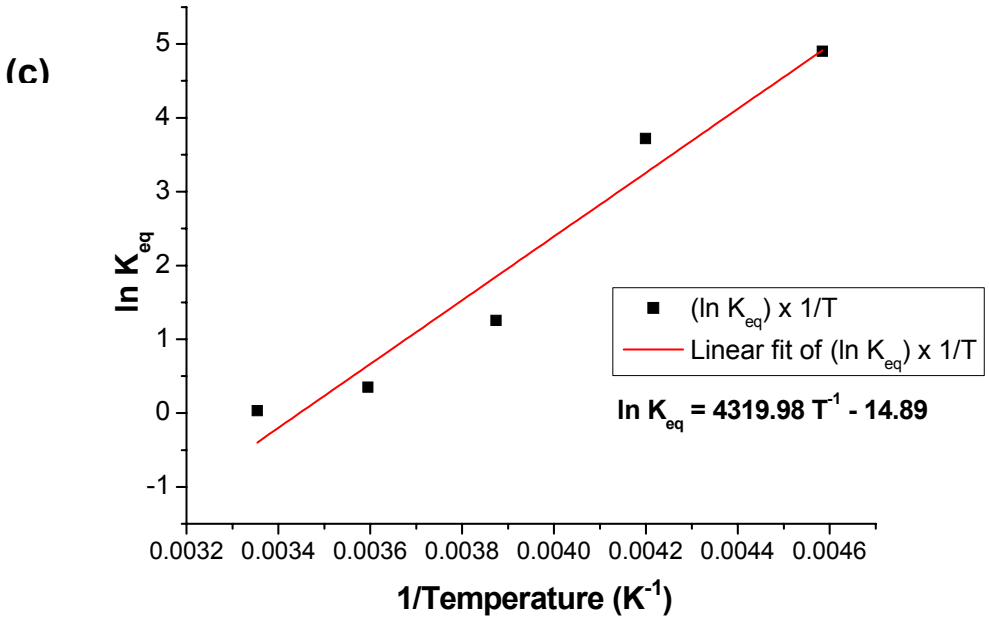

Figure S7 – Van't Hoff's plots for complexes (a) **I**, (b) **N** and (c) **C**.

[1] A. Schweiger and G. Jeschke, *Principles of Pulse Electron Paramagnetic Resonance,* Oxford University Press, New York, 2001.